ARTICLE

doi:10.1038/nature10178

Structural insight into brassinosteroid perception by BRI1

Ji She[1,2,3]*, Zhifu Han[1]*, Tae-Wuk Kim[4], Jinjing Wang[3], Wei Cheng[3], Junbiao Chang[5], Shuai Shi[5], Jiawei Wang[1], Maojun Yang[1], Zhi-Yong Wang[4] & Jijie Chai[1,3]

Brassinosteroids are essential phytohormones that have crucial roles in plant growth and development. Perception of brassinosteroids requires an active complex of BRASSINOSTEROID-INSENSITIVE 1 (BRI1) and BRI1-ASSOCIATED KINASE 1 (BAK1). Recognized by the extracellular leucine-rich repeat (LRR) domain of BRI1, brassinosteroids induce a phosphorylation-mediated cascade to regulate gene expression. Here we present the crystal structures of BRI1(LRR) in free and brassinolide-bound forms. BRI1(LRR) exists as a monomer in crystals and solution independent of brassinolide. It comprises a helical solenoid structure that accommodates a separate insertion domain at its concave surface. Sandwiched between them, brassinolide binds to a hydrophobicity-dominating surface groove on BRI1(LRR). Brassinolide recognition by BRI1(LRR) is through an induced-fit mechanism involving stabilization of two interdomain loops that creates a pronounced non-polar surface groove for the hormone binding. Together, our results define the molecular mechanisms by which BRI1 recognizes brassinosteroids and provide insight into brassinosteroid-induced BRI1 activation.

Ubiquitously distributed throughout the plant kingdom, brassinosteroids are a class of low-abundance phytohormones that have crucial roles in many aspects of growth and development[1,2]. Studies in *Arabidopsis* have led to the identification of a number of genes involved in brassinosteroid perception and signalling[3–9]. One of them, *BRI1*, when mutated, abolishes brassinosteroid-mediated responses of plants[3]. BRI1 belongs to a large family of plant LRR receptor-like kinases (RLKs) with more than 200 members in *Arabidopsis* and over 300 in rice[10]. LRR RLKs are characterized by an extracellular LRR domain, a single-pass transmembrane segment and a cytoplasmic kinase domain. BRI1 has been established as a bona fide receptor of brassinosteroids by genetic and biochemical investigations[3,11,12]. The most convincing evidence for this comes from a biochemical study showing that BRI1(LRR) is essential and sufficient for recognition of brassinosteroids[12]. A 70-residue island domain (residues 587–656) is indispensable for brassinosteroid recognition. Binding of brassinosteroids to BRI1 initiates a phosphorylation-mediated cascade, transducing the extracellular steroid signal to transcriptional programs[13,14].

A second gene named *BAK1* involved in brassinosteroid signalling also encodes an LRR RLK, albeit with only five extracellular LRRs[4,5]. Although not involved in brassinosteroid binding, BAK1 promotes brassinosteroid-induced signalling by physically associating with BRI1 (refs 4, 5, 15). Several models[2,4,5,8,16–19] of brassinosteroid-induced BRI1 activation converge at transphosphorylation within the BRI1–BAK1 complex, which involves brassinosteroid-enhanced BRI1 homodimerization[16], release of BRI1 KINASE INHIBITOR 1 (BKI1)[19] from BRI1, and BRI1–BAK1 heterodimerization[17–19]. It is still not fully understood how brassinosteroids are perceived by BRI1 to give rise to these events.

In the present study, we report the crystal structures of free BRI1(LRR) and its complex with brassinolide (the most active form of brassinosteroid) (Supplementary Table 1). The structures not only reveal the molecular mechanisms underlying brassinosteroid recognition by BRI1 and provide insight into brassinosteroid-induced BRI1 activation, but also explain the structure–activity relationship of brassinosteroids and serve as a foundation for the rational design of nonsteroidal mimetics.

A helical solenoid structure of BRI1(LRR)

The three-dimensional structure of brassinolide-free BRI1(LRR) (residues 30–589, 596–643 and 647–772) contains 25 LRRs as predicted[3], including 24 regular ones and an irregular one abutting the amino-terminal side. The LRRs packed in tandem assemble into a highly curved solenoid structure (Fig. 1a), with the overall rotation angle about the central axis approximately 360 degrees (Fig. 1b). Compared to the regular horseshoe-shaped structures of other LRR proteins, one notably distinct feature of the BRI1(LRR) structure is that it is exceptionally twisted, resulting in formation of a whole turn of right-handed helix with an inner diameter of about 30 Å. Relative to LRR1, LRR25 shifts about 60 Å along the central axis of the helix (Fig. 1a). An unprecedented structural feature of BRI1(LRR) is that it has an insertion domain anchored to the inner surface of the solenoid and running across six LRRs (Fig. 1a). The N-terminal capping domain (residues 30–70), consisting of one β strand (β1) and two α helices, is integrated into the LRR structure by forming an anti-parallel β sheet with the β strand from the irregular repeat, whereas the carboxy-terminal capping domain (residues 752–772) uses two short helices to tightly pack against the last repeat (Fig. 1a). Eight potential glycosylation sites (Supplementary Fig. 2) as defined by sufficient electron density were found in BRI1(LRR). An assignment of functions to them awaits further investigations.

Like canonical LRR proteins, the concave surface of the BRI1(LRR) solenoid is composed of a parallel β sheet comprising 25 continuously running parallel β strands. Compared to many other LRR proteins, however, BRI1(LRR) also possesses parallel but distorted β sheets following the inner β structure in most of the repeats (Fig. 1a, b). This is probably due to the plant-specific consensus sequence L/fXGxI/vP (X and x stand for polar and any amino acid, respectively)[20] of BRI1(LRR)s (Supplementary Fig. 2) found in many LRR RLKs, as a similar structural

[1]Key Laboratory for Protein Sciences of Ministry of Education School of Life Sciences, Tsinghua University, Beijing 100084, China. [2]College of Biological Sciences, Peking University, Beijing 100084, China. [3]National Institute of Biological Sciences, No. 7 Science Park Road, Beijing 102206, China. [4]Department of Plant Biology, Carnegie Institution for Science, Stanford, California 94305, USA. [5]Department of Chemistry, Zhengzhou University, Zhengzhou 450001, China.
*These authors contributed equally to this work.

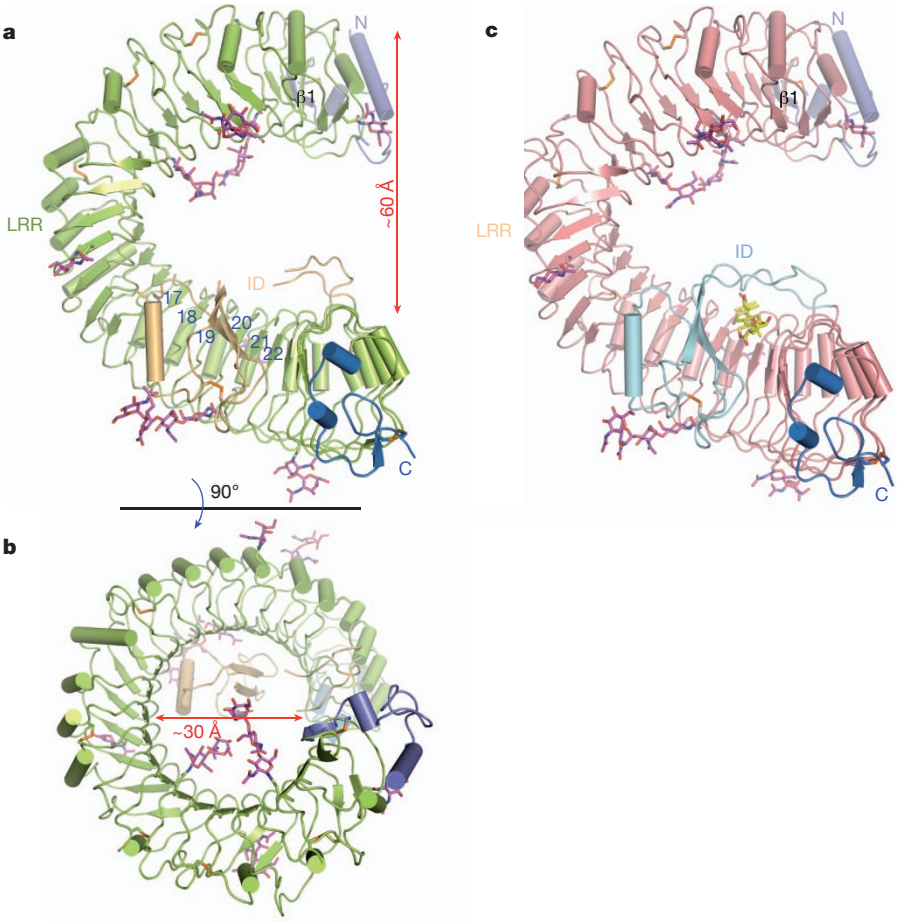

Figure 1 | BRI1(LRR) has a helical solenoid structure. **a**, **b**, Overall structures of brassinolide-free BRI1(LRR) shown in two different orientations. The N-linked sugars (N-acetylglucosamines) are shown in magenta stick representation. Coloured in orange are disulphide bonds. ID, insertion domain. The N- and C-terminal cap is shown in slate grey and marine blue, respectively. The blue numbers in **a** indicate the positions of LRRs. The β strand (β1) from the N-terminal cap is labelled. **c**, Overall structure of brassinolide-bound BRI1(LRR) with the same orientation as **a**. Brassinolide molecule is shown in stick representation and coloured in yellow.

feature also exists in the plant LRR protein PGIP2 (ref. 21). In contrast with the concave side, the convex outer surface consists of varied second structure elements, including 3_{10} helices, α helices and different length of loops (Fig. 1a, b). Some of the loops are stabilized through disulphide bonds formed between two consecutive repeats (LRR2–LRR3, LRR5–LRR6, LRR7–LRR8, LRR10–LRR11 and LRR14–LRR15) (Fig. 1a and Supplementary Fig. 1). The overall structure of BRI1(LRR) (residues 30–775) remains nearly unchanged on brassinolide binding, with a root mean squared deviation (r.m.s.d.) of 0.70 Å over 734 Cα atoms. The brassinolide molecule is sandwiched between the insertion domain and the concave surface of the solenoid structure (Fig. 1c).

Interruption of BRI1(LRR)s by a folded domain

Two short segments (residues 590–595 and 644–646) from the insertion domain do not have interpretable electron density in the structure of brassinolide-free BRI1(LRR) but become well defined after brassinolide binding (Supplementary Fig. 3). Residues 596–643 form a separate folded domain that consists of one three-stranded antiparallel β sheet and one 3_{10} helix (Fig. 2a). In addition, this domain contains one disulphide bridge (Cys 609–Cys 635) that can further contribute to its structural integrity. A database search using the Dali server (http://ekhidna.biocenter.helsinki.fi/dali_server) did not reveal known structures that share significant homology with the insertion domain, indicating that it represents a novel fold.

Extensive non-covalent interactions including van der Waals and polar interactions exist between the insertion domain and the solenoid structure. While making few contacts with the remaining parts of the insertion domain, the 3_{10} helix packs tightly against Phe 449 and Leu 473 from underneath and forms a large network of hydrogen bonding interactions with those from one flanking side (Fig. 2b). In contrast with the 3_{10} helix, β36 primarily binds the concave surface (Fig. 2a). Around this binding site, Trp 516, Ile 540, Trp 564 and Phe 658 establish close contacts with one side of β36, whereas Trp 472 and Phe 497 wedge between β36 and the 3_{10} helix (Fig. 2b). Hydrogen bonds dominate the interactions of the loop linking the 3_{10} helix and β36 with the concave surface. Additionally, packing of the carbonhydrate moiety of the glycosylated Asn 545 against the loop connecting the 3_{10} helix and β37 seems to have a role in positioning the insertion domain in the concave surface (Fig. 2a). Two mutations, G613S and S662F, generated weak hormone-insensitive phenotypes[2]. Our structure indicates that they can perturb local conformations and consequently generate a deleterious effect on BRI1 recognition of brassinosteroids. Substitution of Gly 613 with serine would produce steric clash with the carbonyl oxygen of Ile 600 or the benzene ring of Tyr 599 and consequently generate a damaging effect on the β sheet of the insertion domain (Supplementary Fig. 4). Ser 662 is limited within a small pocket and its mutation to the bulky residue phenylalanine is expected to generate serious clash with its neighbouring residues, in particular the Gly 611 that is N terminal to β36.

Brassinolide binds to a surface groove on BRI1(LRR)

We used ^{3}H-labelled brassinolide to test if the purified recombinant BRI1(LRR) was active in binding brassinolide. As shown in Fig. 3a, the protein showed a comparable brassinolide-binding activity to that

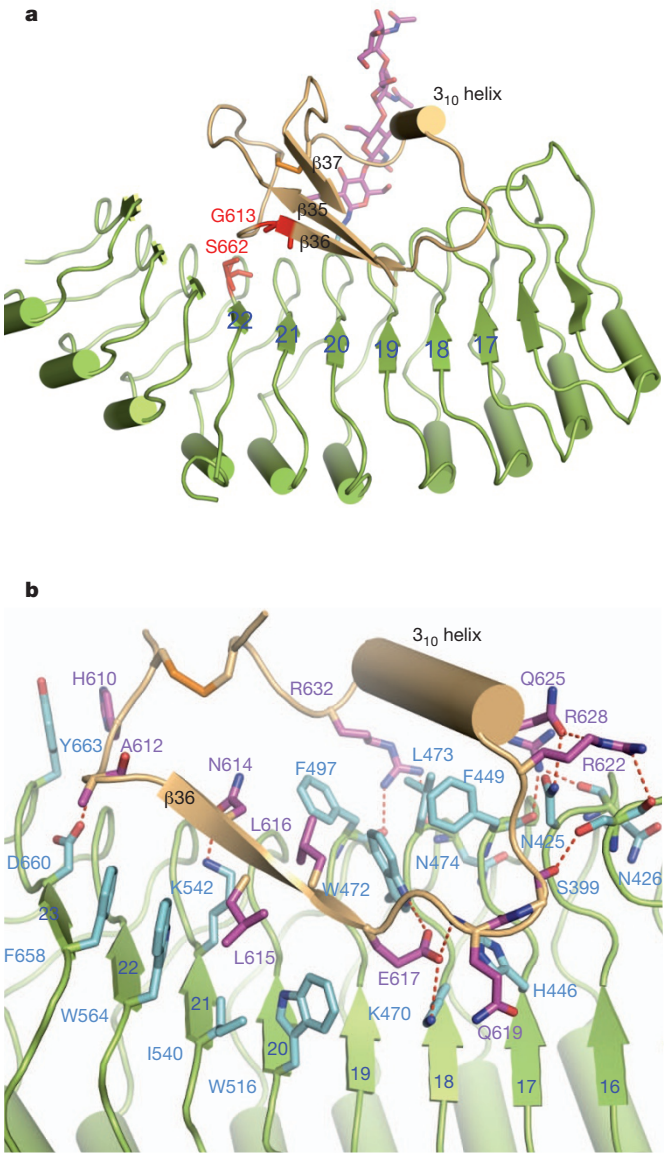

Figure 2 | Interaction of the insertion domain with LRRs. **a**, Cartoon representation of BRI1(LRR) highlighting interaction of the insertion domain with the concave surface. The positions of two genetic mutants are shown in red and stick representation. **b**, Detailed interactions of the insertion domain with LRRs. The side chains from the insertion domain are shown and labelled in purple, and those from LRRs in cyan. Red dashed lines represent hydrogen bonds.

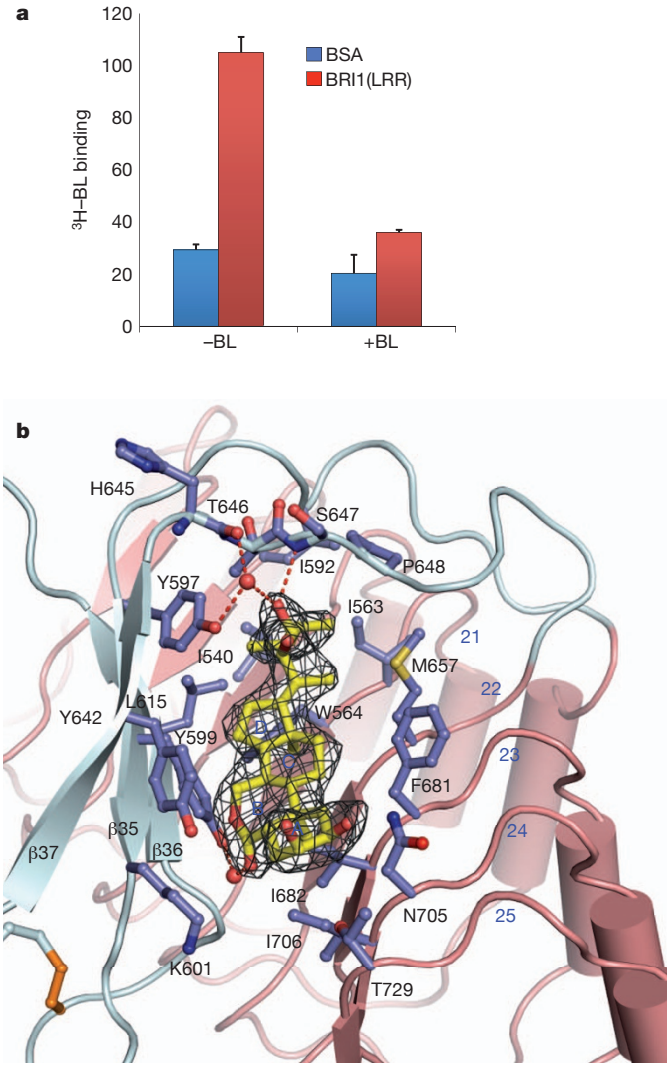

Figure 3 | Brassinolide binds a hydrophobic groove between the insertion domain and the inner surface of LRRs. **a**, ^{3}H-brassinolide (^{3}H-BL) binding activity of BRI1(LRR). About 1 mg ml^{-1} BRI1(LRR)–His (red bar) or bovine serum albumin (BSA) as control (blue bar) was incubated with 20 nM ^{3}H-brassinolide in the absence (−BL) or presence (+BL) of 20 μM unlabelled brassinolide. BRI1-bound ^{3}H-brassinolide was recovered using nickel beads and quantified by scintillation counting. Data represent the average of triplicate assays and error bars are standard deviations. **b**, Detailed interactions between brassinolide and BRI1(LRR). Shown in mesh is omit electron density (2.5δ) around brassinolide. The insertion domain and LRRs are coloured in slate grey and salmon pink, respectively. The side chains from both the insertion domain and LRRs are shown in slate grey. Red spheres represent oxygen atoms of water molecules. The three β strands from the insertion domain are labelled.

previously reported[12]. In the brassinolide-bound BRI1(LRR) structure, the electron density unambiguously defines the brassinolide molecule that binds to a pronounced hydrophobic groove between the insertion domain and the concave side of the solenoid (Fig. 3b). Most of the residues lining the surface groove are hydrophobic and highly conserved (Supplementary Fig. 1). The fused ring moiety of brassinolide (Supplementary Fig. 5) occupies most of the surface groove (Fig. 3b). The A ring (see Supplementary Fig. 5) makes marginal contacts with the concave surface, whereas the B ring tightly stacks Tyr 642 from one lateral side. The other two rings are sandwiched between Phe 681 and Tyr 599. Despite a smaller size, the two methyl groups C18 and C19 form much denser hydrophobic interactions with BRI1 by docking into two cavities at the bottom. In contrast, the other side of the fused ring is nearly solvent exposed (Fig. 3b). Although extensive shape complementarities exist between brassinolide and the base of the surface groove, a water molecule fills the cavity that is sealed from the solvent region by Lys 601, bridging a hydrogen bond between the carbonyl oxygen at C6 and the hydroxyl group of Tyr 599. Standing in contrast with the fused ring, the distal carbon atoms C24–C28 of the side chain are completely buried into a hydrophobic pocket (Fig. 3b). Further reinforcing the interactions around this contact interface, the hydroxyl group at C23 establishes a hydrogen bond with the backbone nitrogen of Ser 647 and two water-mediated hydrogen bonds with the carbonyl oxygen atoms of His 645 and the hydroxyl group of Tyr 597.

Induced-fit brassinolide recognition by BRI1(LRR)

The crystals of both free and brassinolide-bound BRI1(LRR)s contain one protein molecule per asymmetric unit and have nearly identical packing. This indicates that homodimers formed by two crystallographic symmetry-related molecules (Supplementary Fig. 6) result from crystal packing rather than brassinolide binding. Consistently,

gel filtration assays showed that BRI1(LRR) was monomeric in solution and its apparent molecular weight was not affected by the presence of brassinolide (Fig. 4a). The latter is consistent with the observation[22] that brassinolide had no effect on BRI1 homodimerization in protoplasts. Structural comparison revealed that upon brassinolide binding marked local structural rearrangement occurs to the two loops linking the insertion domain and the LRR structure (referred to as interdomain loops) (Fig. 4b). Brassinolide-induced stabilization of the interdomain loops results in formation of a more marked surface groove where brassinolide binds (Fig. 4c), showing that brassinolide recognition by BRI1(LRR) is a process of induced fit.

Discussion

The hydrophobicity-dominating brassinolide-binding surface groove (Fig. 4c, right) indicates that BRI1(LRR) may be accommodating in ligand binding. This would afford an explanation for why BRI1 is able to respond to a variety of brassinolide derivatives[23]. BRI1 ligand selectivity, on the other hand, can be conferred by the distal polar groups involved in hydrogen bonding interactions as well as the actual shape of the hormone-binding groove. The structural mechanism of brassinolide recognition by BRI1(LRR) rationalizes (Supplementary Fig. 7) the data on the structure–activity relationship of brassinosteroids accumulated during the past decades[23], thus opening new perspectives for designing and developing nonsteroidal mimetic of brassinosteroids with low cost that can be widely applied in agricultural practice.

Our structural analyses reveal that, although the overall structure of BRI1(LRR) remains nearly unchanged upon brassinolide binding, significant structural rearrangement occurs to the interdomain loops around the brassinolide-binding site (collectively referred to as the brassinolide-created surface), which should be associated with brassinosteroid-induced signalling. It is not clear how this region contributes to brassinosteroid-initiated signalling, but it is probably involved in stabilization[16] of the kinase-domain-mediated BRI1 homodimers[19]. The absence of an effect of brassinolide on BRI1 homodimerization in the current study may be due to the isolated ectodomain used for assays or requirement of another protein or peptide, as indicated by the suppression of *bri1* mutants by a secreted peptidase[24]. If this is the case, BRI1 would be different from Toll-like receptors, in which ligand-induced homodimerization for activation can be recapitulated through their isolated extracellular domains[25,26]. Stabilization of BRI1 homodimers by the brassinolide-created surface is expected to initially activate BRI1 kinase to a basal level, resulting in tyrosine phosphorylation and disassociation of BKI1 (ref. 19); dissociation of BKI1 allows stable association and sequential reciprocal phosphorylation between the kinase domains of BRI1 and BAK1, fully activating the BRI1 kinase as proposed by the sequential phosphorylation model[18]. Alternatively, brassinolide binding may initiate signalling by altering an interaction between the extracellular domains of BRI1 and BAK1. A role of the extracellular domain of BAK1 in brassinosteroid signalling has been indicated by the observations that mutations in this domain of BAK1 affect brassinosteroid sensitivity[27]

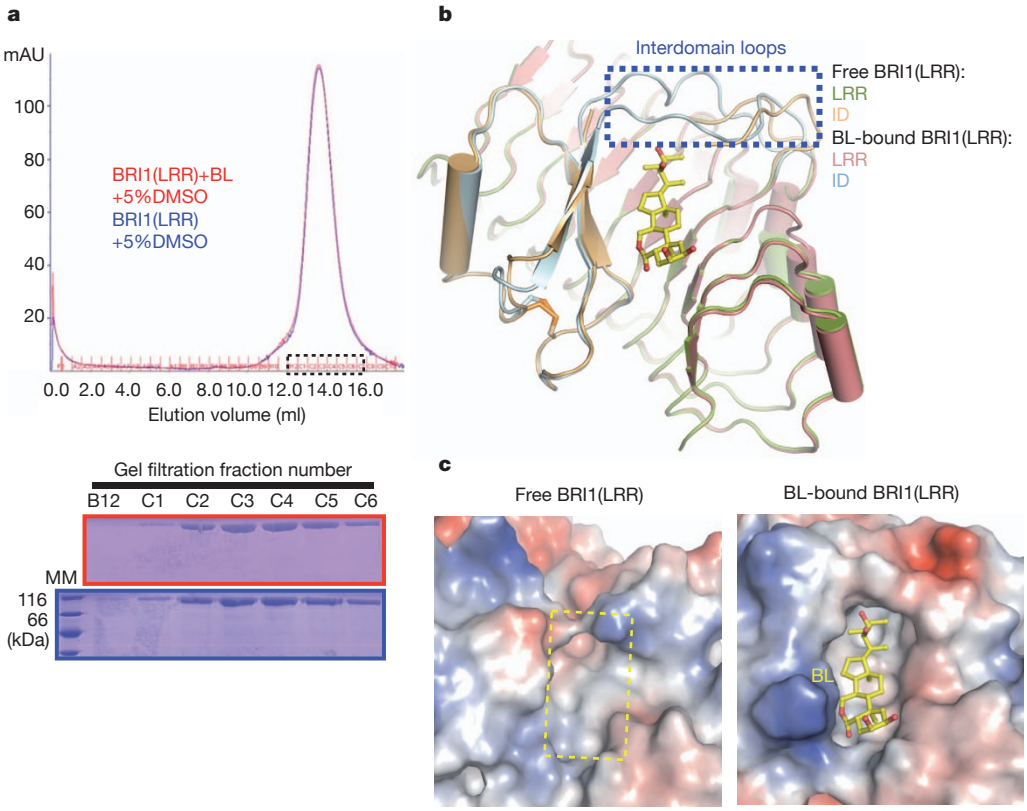

Figure 4 | Brassinolide induces stabilization of two interdomain loops but no dimerization of BRI1(LRR). **a**, Brassinolide (BL) has no effect on the oligomeric status of BRI1(LRR) in solution. Top, superposition of the gel filtration chromatograms of BRI1(LRR) in the absence (blue) and presence (red) of brassinolide. The vertical and horizontal axes represent ultraviolet absorbance ($\lambda = 280$ nm) and elution volume, respectively. Peak fractions are highlighted within the dashed square. The apparent molecular weight of BRI1(LRR) was 109.4 kDa in the presence or absence of brassinolide, higher than the theoretical BRI1(LRR) monomer (83 kDa), probably owing to the existence of multiple glycosylation sites in BRI1(LRR). DMSO, dimethylsulphoxide. Bottom, Coomassie blue staining of the peak fractions shown in the top of the panel after SDS–PAGE. MM, molecular mass marker. **b**, Brassinolide binding induces stabilization of two interdomain loops. Structural superimposition of the free and brassinolide-bound BRI1(LRR) around the brassinolide-binding site. **c**, Brassinolide binding generates a marked hydrophobic surface groove on BRI1(LRR). Shown on the left and right are the electrostatic surfaces of free BRI1(LRR) and brassinolide-bound BRI1(LRR) (shown in the same orientation) around the brassinolide-binding site, respectively. The area highlighted with the yellow dashed square on the left panel is the brassinolide-binding site. White, blue and red indicate neutral, positive and negative surfaces, respectively.

and interaction with BRI1[28]. Although stable BRI1–BAK1 association is a consequence of initial BRI1 activation[19], a possible role of BAK1 and its homologues in initial BRI1 activation has not been excluded by genetic studies; for example, it remains unclear whether mutations of BAK1 and its homologues affect brassinolide-induced BKI1 phosphorylation by BRI1. It is interesting to note that BAK1 has five LRRs and that the new brassinolide-created surface is also located about five LRRs from the membrane surface. Thus, it is also possible that the brassinolide-created surface is involved in interaction with BAK1(LRR), which triggers BRI1 phosphorylation of BKI1 through unknown mechanisms, allowing formation of more stable BRI1–BAK1 receptor complexes. Although the brassinolide-created surface is proposed to be involved in BRI1(LRR) homodimerization or heterodimerization with BAK1(LRR), further studies are needed to determine if brassinosteroids initiate signalling through promoting protein–protein interactions, as many other plant hormones do[29,30].

METHODS SUMMARY

The extracellular domain (residues 24–784) of *Arabidopsis* BRI1 fused with 6×His at the C terminus was expressed with high five cells and a baculovirus expression system. Protein was harvested from the media and purified using Ni-NTA followed by size-exclusion chromatography (Superdex200 10/300 GL column; GE Healthcare). Crystals of free BRI1 and brassinolide-bound BRI1 were grown using the hanging-drop vapour-diffusion method and their structures were determined using molecular replacement. ^{3}H-labelled brassinolide binding assay was performed as previously described[12].

Full Methods and any associated references are available in the online version of the paper at www.nature.com/nature.

Received 10 February; accepted 6 May 2011.
Published online 12 June 2011.

1. Clouse, S. D. & Sasse, J. M. BRASSINOSTEROIDS: essential regulators of plant growth and development. *Annu. Rev. Plant Physiol. Plant Mol. Biol.* **49,** 427–451 (1998).
2. Vert, G., Nemhauser, J. L., Geldner, N., Hong, F. & Chory, J. Molecular mechanisms of steroid hormone signaling in plants. *Annu. Rev. Cell Dev. Biol.* **21,** 177–201 (2005).
3. Li, J. & Chory, J. A putative leucine-rich repeat receptor kinase involved in brassinosteroid signal transduction. *Cell* **90,** 929–938 (1997).
4. Li, J. *et al.* BAK1, an *Arabidopsis* LRR receptor-like protein kinase, interacts with BRI1 and modulates brassinosteroid signaling. *Cell* **110,** 213–222 (2002).
5. Nam, K. H. & Li, J. BRI1/BAK1, a receptor kinase pair mediating brassinosteroid signaling. *Cell* **110,** 203–212 (2002).
6. Li, J. & Nam, K. H. Regulation of brassinosteroid signaling by a GSK3/SHAGGY-like kinase. *Science* **295,** 1299–1301 (2002).
7. Sun, Y. *et al.* Integration of brassinosteroid signal transduction with the transcription network for plant growth regulation in *Arabidopsis*. *Dev. Cell* **19,** 765–777 (2010).
8. Wang, X. & Chory, J. Brassinosteroids regulate dissociation of BKI1, a negative regulator of BRI1 signaling, from the plasma membrane. *Science* **313,** 1118–1122 (2006).
9. Tang, W. *et al.* BSKs mediate signal transduction from the receptor kinase BRI1 in *Arabidopsis*. *Science* **321,** 557–560 (2008).
10. Shiu, S. H. *et al.* Comparative analysis of the receptor-like kinase family in *Arabidopsis* and rice. *Plant Cell* **16,** 1220–1234 (2004).
11. He, Z. *et al.* Perception of brassinosteroids by the extracellular domain of the receptor kinase BRI1. *Science* **288,** 2360–2363 (2000).
12. Kinoshita, T. *et al.* Binding of brassinosteroids to the extracellular domain of plant receptor kinase BRI1. *Nature* **433,** 167–171 (2005).
13. Li, J. Brassinosteroid signaling: from receptor kinases to transcription factors. *Curr. Opin. Plant Biol.* **8,** 526–531 (2005).
14. Kim, T. W. & Wang, Z. Y. Brassinosteroid signal transduction from receptor kinases to transcription factors. *Annu. Rev. Plant Biol.* **61,** 681–704 (2010).
15. Russinova, E. *et al.* Heterodimerization and endocytosis of *Arabidopsis* brassinosteroid receptors BRI1 and AtSERK3 (BAK1). *Plant Cell* **16,** 3216–3229 (2004).
16. Wang, X. *et al.* Autoregulation and homodimerization are involved in the activation of the plant steroid receptor BRI1. *Dev. Cell* **8,** 855–865 (2005).
17. Wang, X. *et al.* Identification and functional analysis of *in vivo* phosphorylation sites of the *Arabidopsis* BRASSINOSTEROID-INSENSITIVE1 receptor kinase. *Plant Cell* **17,** 1685–1703 (2005).
18. Wang, X. *et al.* Sequential transphosphorylation of the BRI1/BAK1 receptor kinase complex impacts early events in brassinosteroid signaling. *Dev. Cell* **15,** 220–235 (2008).
19. J aillais, Y. *et al.* Tyrosine phosphorylation controls brassinosteroid receptor activation by triggering membrane release of its kinase inhibitor. *Genes Dev.* **25,** 232–237 (2011).
20. Kajava, A. V. Structural diversity of leucine-rich repeat proteins. *J. Mol. Biol.* **277,** 519–527 (1998).
21. Di Matteo, A. *et al.* The crystal structure of polygalacturonase-inhibiting protein (PGIP), a leucine-rich repeat protein involved in plant defense. *Proc. Natl Acad. Sci. USA* **100,** 10124–10128 (2003).
22. Hink, M. A., Shah, K., Russinova, E., de Vries, S. C. & Visser, A. J. Fluorescence fluctuation analysis of *Arabidopsis thaliana* somatic embryogenesis receptor-like kinase and brassinosteroid insensitive 1 receptor oligomerization. *Biophys. J.* **94,** 1052–1062 (2008).
23. Zullo, M. T. A. & Adam, G. Brassinosteroid phytohormones—structure, bioactivity and applications. *Braz. J. Plant Physiol.* **14,** 143–181 (2002).
24. Li, J., Lease, K. A., Tax, F. E. & Walker, J. C. BRS1, a serine carboxypeptidase, regulates BRI1 signaling in *Arabidopsis thaliana*. *Proc. Natl Acad. Sci. USA* **98,** 5916–5921 (2001).
25. Liu, L. *et al.* Structural basis of Toll-like receptor 3 signaling with double-stranded RNA. *Science* **320,** 379–381 (2008).
26. Park, B. S. *et al.* The structural basis of lipopolysaccharide recognition by the TLR4–MD-2 complex. *Nature* **458,** 1191–1195 (2009).
27. Whippo, C. W. & Hangarter, R. P. A brassinosteroid-hypersensitive mutant of BAK1 indicates that a convergence of photomorphogenic and hormonal signaling modulates phototropism. *Plant Physiol.* **139,** 448–457 (2005).
28. Yun, H. S. *et al.* Analysis of phosphorylation of the BRI1/BAK1 complex in *Arabidopsis* reveals amino acid residues critical for receptor formation and activation of BR signaling. *Mol. Cells* **27,** 183–190 (2009).
29. Sheard, L. B. & Zheng, N. Plant biology: signal advance for abscisic acid. *Nature* **462,** 575–576 (2009).
30. Sheard, L. B. *et al.* Jasmonate perception by inositol-phosphate-potentiated COI1–JAZ co-receptor. *Nature* **468,** 400–405 (2010).

Supplementary Information is linked to the online version of the paper at www.nature.com/nature.

Acknowledgements We thank S. Huang and J. He at Shanghai Synchrotron Radiation Facility (SSRF) for assistance with data collection; J. Chory from the Salk Institute for providing the tritium-labelled brassinolide. This research was funded by the National Outstanding Young Scholar Science Foundation of National Natural Science Foundation of China grant no. 20101331722 to J. Chai and NIH R01GM066258 to Z.-Y.W.

Author Contributions J. Chai, Z.H., J.S. and Z.-Y.W. designed the experiments. The binding assay was performed by T.-W.K. and the other assays by J.S., Z.H., Jinjing W., W.C., Jiawei W., M.Y., S.S. and J. Chang. Data were analysed by J. Chai, Z.H., J.S. and Z.-Y.W. J. Chai, Z.-Y.W. and Z.H. wrote the paper.

Author Information The atomic coordinates and structure factors of BRI1(LRR) and the BRI1(LRR)–brassinolide complex have been deposited in the Protein Data Bank under the accession codes 3RGX and 3RGZ, respectively. Reprints and permissions information is available at www.nature.com/reprints. The authors declare no competing financial interests. Readers are welcome to comment on the online version of this article at www.nature.com/nature. Correspondence and requests for materials should be addressed to J. Chai (chaijj@mail.tsinghua.edu.cn).

METHODS

Protein expression and purification. The LRR domain of BRI1 (residues 24–784) from *Arabidopsis* with an engineered C-terminal 6×His tag was generated by standard PCR-based cloning strategy and its identity was confirmed by sequencing. The protein was expressed in high five cells using the vector pFastBac 1 (Invitrogen) with a modified N-terminal Hemolin peptide. One litre of cells (2.0×10^6 cells ml^{-1}) was infected with 20 ml baculovirus using a multiplicity of infection of 4 at 22 °C, and protein was harvested from the media after 48 h. The protein was purified using Ni-NTA (Novagen) and size-exclusion chromatography (Superdex 200, Pharmacia) in buffer (10 mM Tris, pH 8.0, 100 mM NaCl). Samples from relevant fractions were applied to SDS–PAGE and visualized by Coomassie blue staining. Protein purification was performed at 4 °C. For crystallization of BRI1(LRR), the purified protein was concentrated to about 3.0 mg ml^{-1} in buffer containing 10 mM Tris, pH 8.0, 100 mM NaCl.

Crystallization, data collection, structure determination and refinement. Crystals of BRI1(LRR) were generated by mixing the protein with an equal amount of well solution (1 µl) by the hanging-drop vapour-diffusion method. A mixture of BRI1(LRR) and brassinolide with a molar ratio of 1:10 was used for generating crystals of their complex. The initial buffer producing crystals of both free BRI1(LRR) and brassinolide-bound BRI1(LRR) contained 0.2 M Na_2SO_4 and 20% (w/v) polyethylene glycol (PEG) 3,350, which was further optimized by adding 10 mM trimethylamine-HCl. Crystals grew to their maximum size ($0.1 \times 0.1 \times 0.1$ mm^3) within 10 days at room temperature (20 °C).

All the diffraction data sets were collected at the Shanghai Synchrotron Radiation Facility (SSRF) at beam line BL17U1 using a CCD detector. Crystals of both brassinolide-free and brassinolide-bound BRI1(LRR) belong to space group C2 with one protein molecule per asymmetric unit. For data collection, the crystals were equilibrated in a cryoprotectant buffer containing reservoir buffer plus 20.0% (v/v) glycerol. The data were processed using HKL2000 (ref. 31). Molecular replacement (MR) with the program PHASER[32] was used to solve the crystal structures of both brassinolide-free and brassinolide-bound BRI1(LRR). The atomic coordinates of PGIP2 (ref. 21) (PDB code 1OGQ) and InlA[33] (PDB code 1O6V) were used as the initial searching model. The model from MR was built with the program COOT[34] and subsequently subjected to refinement by the program PHENIX[35]. The electron density for brassinolide in BRI1(LRR)–brassinolide complex crystal became apparent after refinement of BRI1(LRR). The final refined model contains residues 30–775 of BRI1(LRR) and one brassinolide molecule in brassinolide-bound BRI1(LRR), and residues 30–772 in brassinolide-free BRI1(LRR) except the two segments containing residues 590–595 and 644–646 that have no clear electron density and are presumed to be disordered in solution. The structure figures were prepared using PyMOL[36].

Gel filtration assay. BRI1(LRR) protein purified as described earlier was subjected to gel filtration analysis (Superdex200 10/300 GL column; GE Healthcare) in the presence and absence of brassinolide. Buffer containing 50 mM NaH_2PO_4/Na_2HPO_4 pH 7.4, 100 mM NaCl, 2.0 mM $MgCl_2$ and 5% (v/v) DMSO was used for the assay. A mixture of BRI1(LRR) and brassinolide with a molar ratio of about 1:10 was used to test the effect of brassinolide on the apparent molecular weight of BRI1(LRR). The assays were performed with a flow rate of 0.5 ml min^{-1} and an injection volume of 0.5 ml buffer containing BRI1(LRR) (0.83 mg ml^{-1}) with or without brassinolide at 20 °C. The column was calibrated using five standard proteins, β-amylase 200 kDa, alcohol dehydrogenase 150 kDa, albumin 66 kDa, carbonic anhydrase 29 kDa and cytochrome C 12.4 kDa, which had elution volumes (V_e) of 12.53 ml, 13.25 ml, 14.25 ml, 16.18 ml and 16.97 ml, respectively, under the conditions of assay. The void volume (V_o) for the column used was determined to be 8.15 ml using fresh blue dextran solution (1.0 mg ml^{-1}). The calibration curve of the gel-phase distribution coefficient (K_{av}) versus log molecular weight (M) was obtained using Excel. $K_{av} = (V_e - V_o)/(V_c - V_o)$, where V_e is the elution volume, V_o is the void volume, V_c is the geometric column volume, 24 ml for the column used. The elution volume of BRI1(LRR) in the presence and absence of brassinolide was 13.63 ml under the conditions of assay, corresponding to an apparent molecular weight of 109.4 kDa based on the calibration equation $K_{av} = -0.2366 \lg M + 1.538$, $R^2 = 0.9814$.

^{3}H-labelled brassinolide-binding assay. His-tagged BRI1(LRR), or BSA as control, was incubated with 20 nM ^{3}H-brassinolide, or 20 nM ^{3}H-brassinolide mixed with 20 µM non-radiolabelled brassinolide as competitor, and nickel beads in the brassinolide-binding buffer (0.25 M mannitol, 10 mM Tris-2-[N-morpholino] ethanesulphonic acid (MES), pH 5.7, 5 mM $MgCl_2$, 0.1 mM $CaCl_2$) for 30 min. The beads were washed three times, and His–BRI1(LRR) and bound [^{3}H]-brassinolide were eluted by using 1 M imidazole. The eluted radioactivity was measured by scintillation counter.

31. Otwinowski, Z., &. Minor, W. Processing of X-ray diffraction data collected in oscillation mode. *Methods Enzymol.* **276,** 307–326 (1997).
32. McCoy, A. J. *et al.* Phaser crystallographic software. *J. Appl. Cryst.* **40,** 658–674 (2007).
33. Schubert, W. D. *et al.* Structure of internalin, a major invasion protein of *Listeria monocytogenes*, in complex with its human receptor E-cadherin. *Cell* **111,** 825–836 (2002).
34. Emsley, P. & Cowtan, K. Coot: model-building tools for molecular graphics. *Acta Crystallogr. D* **60,** 2126–2132 (2004).
35. Adams, P. D. *et al.* PHENIX: building new software for automated crystallographic structure determination. *Acta Crystallogr. D* **58,** 1948–1954 (2002).
36. DeLano, W. L. PyMOL molecular viewer ⟨http://www.pymol.org⟩ (2002).